ACS OMEGA

Open Access

http://pubs.acs.org/journal/acsodf

Article

Simple and Cost-Effective Quantum Dot Chemodosimeter for Visual Detection of Biothiols in Human Blood Serum†

Vinayakan Ramachandran Nair,* Kulangara Sandeep, Madhavan Shanthil, Santhakumar Dhanya, Aravind Archana, Muthunayagam Vibin, and Hareendran Divyalakshmi

Cite This: *ACS Omega* 2024, 9, 6588−6594

Read Online

ACCESS | Metrics & More | Article Recommendations | Supporting Information

ABSTRACT: An emission "turn-off" chemodosimeter for the naked-eye detection of biothiols using silica-overcoated cadmium selenide quantum dots is developed. Hole scavenging by the thiol group of cysteine, homocysteine, or glutathione on interaction with quantum dots resulted in an instant and permanent emission quenching under physiologically relevant conditions. Also, the emission suppression is so specific that thiols and substituted thiols (methionine and cystine) can easily be distinguished. A pilot experiment for the visual detection of serum thiols in human blood was also conducted. Densitometry analysis proved the potential of this system as a new methodology in clinical chemistry and research laboratories for routine blood and urine analyses using a simple procedure. This method enables one to visually distinguish biothiols and oxidized biothiols, whose ratio plays a crucial role in maintaining "redox thiol status" in the blood.

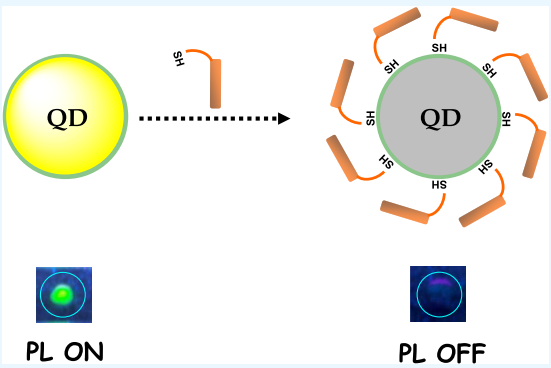

INTRODUCTION

The in vivo maintenance of "redox thiol status", which involves a dynamic system of biothiols and their disulfides, is of great importance for the normal physiological function of the human body. Changes in redox thiol status are a marker of different pathological states and, in turn, several diseases.[1,2] Tailoring simple methods for the clinical analysis of biothiols such as cysteine (Cys), homocysteine (Hcy), and glutathione (GSH) in blood plasma and urine is of particular attention as they play a pivotal role in metabolic processes in living cells by maintaining biological redox homeostasis.[3] For instance, although cysteine residues are relatively rare in proteins, their elevated level in blood is documented as a risk factor for cardiovascular diseases and neurological conditions.[4] Hcy, a key intermediate in methionine metabolism, is found to be a risk factor for disorders including dementia, cardiovascular disease, and Alzheimer's disease.[5,6] Among various peptides, the GSH level in tumor cells is proven to be vital for both protective and pathogenic activity.[7] Also, GSH protects cells from damage by toxic compounds, reactive oxygen compounds, and radiation.[8]

Selective detection and quantification of these biologically important analytes are major difficult tasks due to their structural similarity, incorporating both carboxylic and amino functionalities. Various approaches for qualitative as well as quantitative analysis of these bioanalytes have been developed, mainly based on electroanalytical techniques,[9,10] high-performance liquid chromatography (HPLC),[11,12] capillary electrophoresis separation, immunoassays based on derivatization with fluorescent/phosphorescent reagents, spectrophotometric methods, etc.[13,14] Unfortunately, all of these methods require either expensive reagents or equipment or skilled manpower to ensure reproducibility. In this context, much attention is being paid to the development of simple and cheap fluorescent probes, without compromising selectivity and sensitivity.[15−24] Nanoparticles have been proven to be an efficient substitute for organic fluorophores, particularly for developing emission "turn on/off" sensors.[25−33] Among various nanoparticles, quantum dots (QDs) are of particular interest in developing novel biosensors owing to their unique properties such as broad absorption band, emission in the visible region, photostability, etc.[34−42] Moreover, the potential of QDs to transfer electrons or holes to biologically important molecules, interacting covalently or noncovalently with their surface, can be used to tune the QD emission intensity and thus generate charge transfer-based emission "on/off" signaling.[43−56]

These unique properties of QDs motivated many groups to design, synthesize, and develop QD chemosensors and chemodosimeters from different classes of materials; carbon, graphene, sulfur, $MoSe_2$, and MoS_2 are some of the recently

Received: September 28, 2023
Revised: January 8, 2024
Accepted: January 12, 2024
Published: February 2, 2024

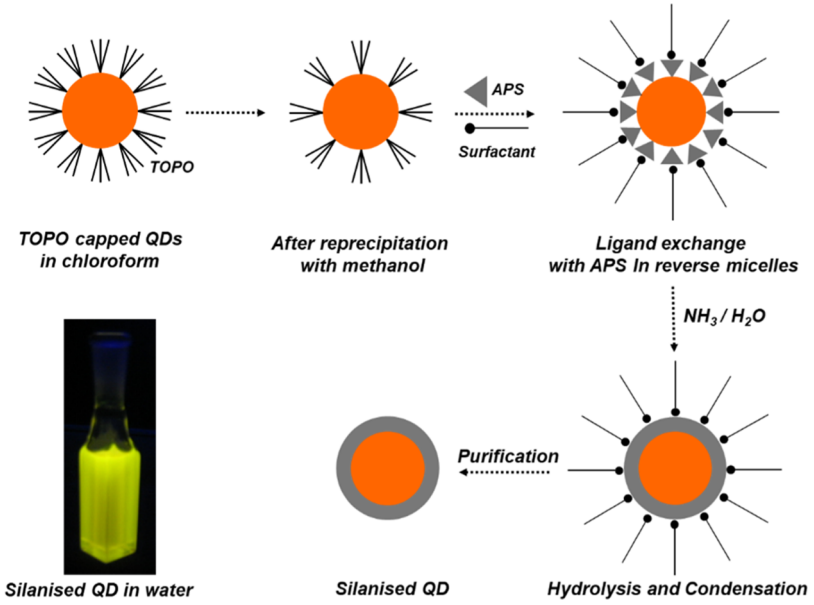

Figure 1. Schematic representation of silanization of TOPO-capped CdSe QDs by the reverse microemulsion method.

reported zero-dimensional materials for the sensing of bioanalytes.[45−51]

While designing QDs for detecting biomolecules, their dispersibility in the biological milieu is a mandatory requirement. Unfortunately, solubilizing QDs in aqueous media by encapsulating in multifunctional capping agents or embedding in a thick siloxane shell restricts the QD core-analyte direct charge transfer process and, in turn, limits their scope in developing biosensors.[57−59] To circumvent this limitation, herein, we report silica-overcoated cadmium selenide QDs (silica-overcoated QDs) with an optimum shell coverage, as an emission "turn-off" sensor, for thiol-containing amino acids and peptides. Although silica-overcoated QDs have been employed for biological labeling and imaging purposes, their biosensing applications are seldom explored.[60,61] Although chemosensors possess a distinct advantage in terms of their reusability, the chemodosimeters reported offer another essential property in terms of high selectivity. To the best of our knowledge, this is the first observation in which silica-overcoated QDs were used for the visual detection of biothiols under physiologically relevant conditions. The advantages of this nanoprobe over some of the other recently reported various nanomaterials for detection of bioanalytes are tabulated in the Supporting Information. The chemodosimeter described herein proves how sulfhydryl containing amino acids like cysteine, homocysteine, and the tripeptide glutathione can be identified directly and instantly by looking at the emission of CdSe QDs illuminated with a hand-held ultraviolet (UV) lamp. We also demonstrate its employability as a testing kit for the naked-eye detection of biothiols in human blood serum.

RESULTS AND DISCUSSION

CdSe QDs capped with trioctylphosphine oxide were synthesized and rendered water-soluble by salinization using aminopropyl silane (APS), following a reverse microemulsion method. The details of the synthesis, salinization process, and evaluation of colloidal properties of QDs have been published elsewhere (Figure 1).[62,63]

Prepared QDs showed excellent solubility and colloidal stability in a phosphate-buffered saline (PBS) buffer (pH 7.3) with strong emission at ∼550 nm. The emission was found to be stable over a wide range of pHs and ionic strengths of the medium (Figure S1). On introducing Cys, the emission intensity of QDs (0.17 μM in phosphate-buffered saline (PBS), pH 7.3, excited at 400 nm) decreased remarkably and instantly, without any change in the emission maximum as well as in the absorption excitonic peaks (Figure 2 inset; see also the link for

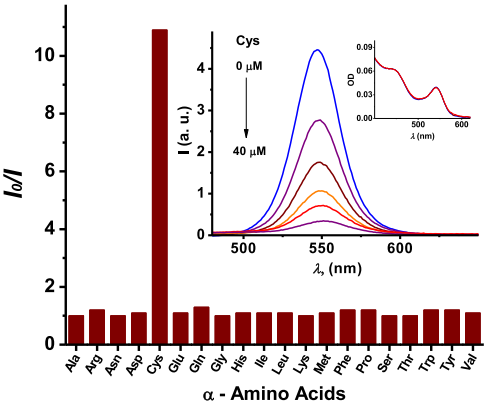

Figure 2. QD emission "turn-off" selectivity of Cys over other natural α-amino acids. Io and I represent emission intensity in the absence and presence of a quencher, respectively. Inset: QD emission (0.17 μM, PBS, pH 7.3, excited at 400 nm) and absorbance spectra in the presence of Cys, when added to 40 μM.

video in the Supporting Information). The permanent suppression of the emission intensity of QDs by Cys, without affecting the absorption profile, indicated that the quenching is affected by a QD-Cys charge transfer process.

Interestingly, except for Cys, none of the other 19 natural α-amino acids displayed the same effect, showing the selectivity of Cys in quenching the QD emission (Figures 2 and S2).

It is relevant to note that the electronic absorbance spectrum of QDs remains unaffected in the presence of Cys (inset of Figure 2). It ruled out the possibility of any nonphotochemical reaction between Cys and QD, which would degrade the electronic integrity of the nanoparticle and might have led to a

https://doi.org/10.1021/acsomega.3c07518
ACS Omega 2024, 9, 6588−6594

reduced emission intensity. A plot of relative emission intensity against the concentration of Cys (Stern−Volmer plot) showed a linear behavior, indicating the presence of a unique mode of emission quenching pathway, by either dynamic or static mechanism (Figure S3A). A time-resolved emission decay analysis of QDs, in the presence of Cys, showed that the decrease in emission quantum yield is not followed by a change in excitonic lifetime (Figure S3B). The average lifetime remained constant (∼22 ns, Table S4), indicating that a static mode of quenching mechanism prevails, where QD forms a nonluminescent complex with Cys (QD-Cys).

Using the Stern−Volmer quenching constant (K_{SV}) 89254 M^{-1}, the bimolecular quenching constant (k_q) was extracted as 4.1×10^{12} M^{-1} s^{-1}. This value is significantly faster than the diffusion-limited rate constant for biomolecules in aqueous media, supporting the above assumption that the quenching is affected via a QD-Cys complex formation.[64,65] Further, we observed exactly the same effect on emission and absorbance of QDs with other thiol-containing biologically important molecules such as homocysteine (Hcy) and glutathione (GSH) under identical conditions (data provided in the Supporting Information). In short, analytes with thiol functionality (−SH) significantly quenched the QD emission in contrast to those with substituted thiols like methionine (−SCH_3) or cystine (−S−S−). It clearly spells out the selectivity and role of the thiol moiety in causing QD emission quenching.

The limit of detection (LOD) and the limit of quantification (LOQ) were determined according to the 3σ IUPAC definition using the following equations: LOD = $3\sigma/K_{sv}$ and LOQ = $10\sigma/K_{SV}$, where K_{sv} is the slope of the linear fit (Stern−Volmer constant) and σ is the standard deviation. The linear regression equation for Cys for a concentration range of 0−40 μM is $y = 89254x + 1.0576$ ($R^2 = 0.9969$), where y refers to Io/I and x is the concentration of Cys. The LOD is calculated to be 0.44 μM, indicating that the proposed probe was highly sensitive to Cys. The corresponding LOQ was estimated as 1.48 μM. Similar calculations gave LOD/LOQ values as 0.65/2.15 μM and 0.87/2.92 μM for Hcy and GSH, respectively.

It is well established by comparing the redox potential of the valence band edge of CdSe QDs and of thiol that the radiative recombination of exciton is hindered by a hole trapping process.[66] In a previous report, Hollingsworth and co-workers showed that it is the "thiolate anion (RS-)" rather than "thiol (RSH)" that comprises the active species in affecting the optical properties of the QD in aqueous media.[67] Seemingly, in the present case also, we can expect small amounts of thiolate anions in equilibrium with corresponding thiols, as the pK_a values of the analytes under consideration (8.3, 9.5, and 8 for Cys, Hcy, and GSH, respectively) are close to the experimental pH conditions (pH ∼ 7.3, PBS).[68,69] From these factors, it is clear that Cys, Hcy, and GSH interact with the CdSe core via the thiolate moiety and quench the emission through a photoinduced charge transfer process.

The feasibility of photoinduced electron transfer from the thiol group to the QD valence band edge was assessed based on donor and acceptor energy levels. The highest occupied molecular orbital (HOMO) and the lowest unoccupied molecular orbital (LUMO) levels of QD were measured by cyclic voltammetry analysis (Figure S10). The band gap was calculated using the following equations

$$E_{HOMO} = -[E^{ox} + 4.71]eV$$

$$E_{LUMO} = -[E^{red} + 4.71]eV$$

Using the above relationships, the HOMO and LUMO levels of CdSe QDs were estimated as −5.85 and −3.95 eV, respectively. From this, the band gap was calculated as 1.9 eV. The position for the standard redox potential of thiol is located at about −5.5 eV. It is clear that the hole formed in the HOMO of excited QD can be scavenged by thiol, as the HOMO energy level of the thiol lies between HOMO and LUMO levels of the QD—an acceptor-excited photoinduced electron transfer (PeT).[70] Besides, many groups reported that thiols would always quench the emission of CdSe, irrespective of the diameter of the nanocrystals, because their redox levels are located above the valence band edge of the QDs and thereby trap photogenerated holes.[71,72]

Besides, the energy balance or the driving force of a photoinduced electron transfer Gibbs free energy associated with the possible PeT process was estimated using the Rehm−Weller equation[64]

$$\Delta G\ (eV) = E_{ox}(D + /D) - E_{red}(A/A\text{-}) - E_{00} + C$$

where ΔG is the free energy change involved, E_{ox} is the oxidation potential of the electron donor (thiol group), E_{red} is the reduction potential of the electron acceptor (QD), E_{00} is the smallest band gap calculated from the absorption onset of QD, and C is a constant that accounts for the energy release due to the charge separation interaction of the charges with the solvent. In the current work, C is considered to be zero as an electrostatic complex exists between QD and thiols before the excitation of QD and subsequent electron/hole transfer occurs. In order to estimate ΔG, we have used the species-specific microscopic standard redox potentials of cysteine, homocysteine, and glutathione. In all three cases, a negative free energy resulted (−0.46 eV for Cys, −0.43 eV for Hcy, and −0.56 eV for GSH; Table S11), confirming the thermodynamic possibility of electron transfer from the thiol to the empty HOMO of QDs.[73]

The role of the silica shell in realizing this process may be visualized in a couple of ways; the analyte approaches the QD core through the porous siloxane shell and binds to the surface via the thiolate moiety, resulting in QD emission quenching. If this was the mechanism, it should be guided by the steric factor of analytes and will be reflected in the bimolecular quenching constant. Although there is a considerable difference in the hydrodynamic radii of analytes (compared to Cys, GSH is a tripeptide), the K_q values of Cys, Hcy, and GSH are almost comparable (Table S5). It clearly rules out the possibility of analyte interaction with the QD core surface by diffusing through the porous silica shell.

High-resolution transmission electron microscopy (HRTEM) of silica-overcoated QDs (Figure S12) showed the presence of a thin silica layer (∼1 nm) over the CdSe core. So it may be anticipated that the silica shell formed may be nonuniform, leaving small voids or pockets on the QD surface, which facilitate the binding of the thiolate group directly onto the CdSe core. To evaluate this assumption, CdSe QDs were overcoated with a thick silica shell using tetraethyl orthosilicate (TEOS) as a silica precursor and repeated emission quenching studies under identical conditions. Thiol-containing analytes showed little effect on the QD emission intensity, which is ascribed to the poor QD core−analyte interaction due to high

https://doi.org/10.1021/acsomega.3c07518
ACS Omega 2024, 9, 6588−6594

silica shell thickness (~15 nm, Figure S12). Moreover, in the case of CdSe QDs overcoated with very excess APS, emission quenching was not observed by biothiols.

Further, we conducted a demonstration of the naked-eye detection of biothiols in water using the silica-overcoated QDs, and the photograph is shown in the inset of Figure 3. An aqueous suspension of QD was placed on a glass slide and illuminated using a hand-held UV lamp. The addition of a drop of aqueous solution of Cys, Hcy, or GSH instantly quenched the emission of QD, enabling a visual detection (a video link is provided in the Supporting Information to watch the live experiment). A similar strategy was extended for the visual detection of biothiols in human blood serum. QDs were diluted with PBS to a final concentration of 0.17 μM, and 10 μL of this solution was dispensed (labeled 1–6) on a glass slide. 1 and 2 served as the control and blank (added PBS alone) experiments, respectively. Serum samples (S1, S2, and S3) were collected from three volunteers and diluted with PBS buffer in the ratios 1:1000, 1:100, 1:10, and 1:2. Equal volumes of these diluted samples were mixed with QDs (3–6, increasing concentration order) on a glass slide.

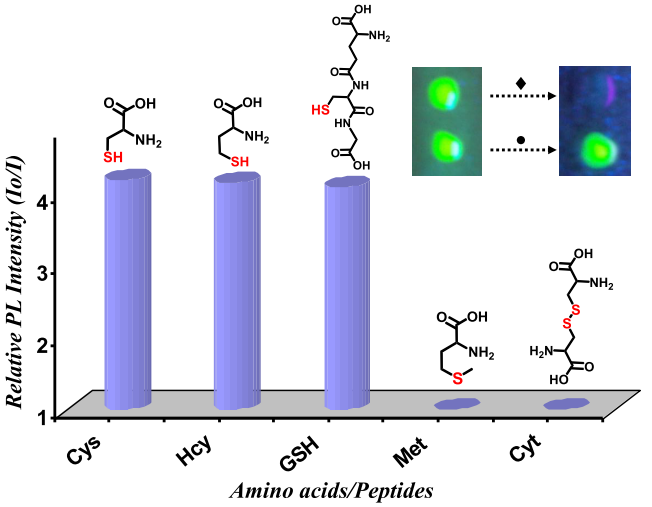

Figure 3. Relative luminescence intensity (Io/I) of silica-overcoated QDs in PBS (pH 7.3) on adding analytes containing a thiol moiety (♦ Cys, Hcy, and GSH). QD emission was instantly quenched in these cases, in contrast to structurally similar analytes (● Met and Cyt). Inset: Photographs illustrating the QD emission "turn-off" effect when the thiol-containing analyte is added (QD drop-cast on a glass slide and illuminated under a UV lamp).

QD emission after mixing serum samples of various concentrations was monitored under UV light using a gel documentation system (UVP, Cambridge, U.K.), and imaging was done using a CCD camera. Photographs recorded under UV illumination after the serum was mixed with QDs are shown in Figure 4. In the case of S1, the emission of QD was not affected by the addition of serum at any concentration level. In contrast, S2 and S3 turned off the emission at higher concentrations. The effect was significant at a dilution of 1:100 in the case of S3 compared to S2, where the same effect was observed at a dilution of 1:10. These results indicate that S3 has a higher "free thiol" content compared to S2, while S1 is free from "free thiols" or may be below the detection limit. More clinical trials with a higher number of serum (and urine) samples are currently under way to explore the viability of commercialization.

CONCLUSIONS

In summary, a novel emission "turn-off" probe based on silica-overcoated QDs for the visual detection of biothiols (cysteine, homocysteine, and glutathione) was developed with detection limits of 0.44, 0.65, and 0.87 μM for Cys, Hcy, and GSH, respectively. The hole trapping by the thiol group resulted in an instant and permanent quenching of the QD emission under physiologically relevant conditions. The system was able to discriminate substituted thiols (methionine and cysteine) from free thiols. A pilot experiment for the visual detection of serum thiols in human blood plasma was also demonstrated. Analysis based on densitometry proved the potential of this system as a new methodology in clinical chemistry or research laboratories for blood and urine analysis. Further experiments

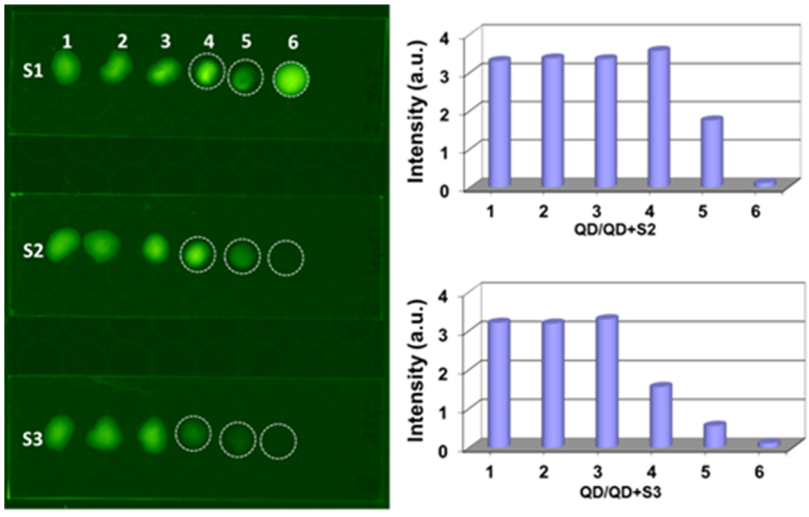

Figure 4. (Left panel) Analysis of human blood serum samples (S1, S2, and S3) using silica-overcoated QDs. 1–6: QD drops (10 μL, 0.17 μM, PBS) on a glass slide. 1 and 2 represent control and blank experiments, respectively. Serum concentration increases from 3 to 6 (diluted with PBS on the order of 1:1000, 1:100, 1:10, and 1:2). In the cases of S2 and S3, the QD emission was turned off at higher serum concentrations (indicated by circles). (Right panel) Graphs obtained from densitometry analysis of photographs corresponding to S2 and S3.

https://doi.org/10.1021/acsomega.3c07518
ACS Omega 2024, 9, 6588–6594

are going on to develop a QD-based tailormade kit for the quantitative and qualitative detection and discrimination of biothiols in clinical laboratories.

MATERIALS AND METHODS

The electronic absorption spectra were recorded on a Shimadzu Model UV-3101 or a 2401 PC UV−vis−NIR scanning spectrophotometer, emission spectra were collected using a SPEX-Fluorolog F112X spectrofluorimeter, photoluminescence lifetimes were measured using an IBH Picosecond single photon counting system with excitation source 440 nm (pulse width <200 ps), and luminescence decay profiles were deconvoluted using IBH data station software V2.1. Fourier transform infrared (FTIR) spectroscopy studies were performed using a Shimadzu IR Presige-21 FTIR spectrometer. X-ray diffraction patterns were recorded using a Philips X'Pert Pro, an X-ray diffractometer with Cu Kα radiation (1.5406 Å), and spectra were analyzed using X'Pert Highscore software. For HRTEM studies, a drop of nanoparticle solution was placed on a carbon-coated Cu grid and the solvent was allowed to evaporate. Specimens were imaged on an FEI Tecnai G^2 S-TWIN 300 kV high-resolution transmission electron microscope. Melting points were determined on a Mel-Temp II melting point apparatus. Blood serum analysis experiments were carried out using a gel documentation system (UVP, Cambridge, U.K.) equipped with a (black and white) CCD camera. Densitometry analysis of the photographs was done using Visionworks LS analysis software.

All of the spectroscopic studies were carried out at ambient and identical conditions (unless specified), where the QD concentration was in the micromolar (~0.17 μM) range and photoluminescence (PL) was collected by exciting at 450 nm (OD ~ 0.05) for all samples. Also, we have accounted for the small dilution effect (<2%) by performing control experiments. Experiments were performed using spectroscopic-grade solvents, double-distilled/deionized water, and PBS (pH 7.3). Reagents used were purchased from Aldrich, Merck, and Fluka and used as such.

EXPERIMENTAL SECTION

Synthesis of TOPO-Capped CdSe QDs. A reaction mixture containing cadmium oxide (0.134 g, 1.04 mM), dodecylamine (7.6 g, 41.4 mM), trioctylphosphine oxide (5.4 g, 13.8 mM), and tetradecylphosphonic acid (0.80 g, 2.8 mM) was heated to 300 °C until cadmium oxide dissolves completely to produce an optically clear solution. Keeping the temperature at 300 °C, an injection mixture containing TOPSe (166 μL, 0.16 mM) and TOP (10.4 mL, 5 mM) was introduced. After the desired crystal growth, the reaction was arrested by reducing the reaction temperature to ambient conditions, and the QDs thus obtained were purified by size-selective precipitation using methanol, followed by centrifugation. QDs were characterized by spectroscopic and HRTEM analyses and the average size of QDs was estimated as 7.1 nm.

Synthesis of Silica-Overcoated CdSe QDs. Cyclohexane (20 mL) was added with a mixture of Igepal CO-520 (2.6 mL) and CdSe QDs (800 μL) along with aminopropyl silane (APS) (126 μL, 0.72 mM) and stirred vigorously for 30 min under an inert atmosphere. Then, ammonia solution (300 μL, 33 wt %) was added, and the stirring was continued for 24 h. The silanized QDs were precipitated as globules, which were further purified by washing with dry chloroform (8 mL) 5 times to remove unreacted components and then redissolved in PBS (pH 7.3). Igepal CO-520 (2.6 mL) was dissolved in cyclohexane (20 mL) by stirring under an inert atmosphere for 30 min.

ASSOCIATED CONTENT

Supporting Information

The Supporting Information is available free of charge at https://pubs.acs.org/doi/10.1021/acsomega.3c07518.

Characterization and stability study of QDs; luminescence quenching studies with amino acids and glutathione; and cyclic voltammetric studies (PDF)

AUTHOR INFORMATION

Corresponding Author

Vinayakan Ramachandran Nair − *Department of Chemistry (Research Center under MG University, Kerala), NSS Hindu College (Nationally Accredited with 'A' Grade), Changanacherry 686102 Kerala, India; Chemical Sciences and Technology Division, National Institute for Interdisciplinary Science and Technology (NIIST-CSIR), Thiruvananthapuram 695019 Kerala, India;* orcid.org/0000-0003-0082-3659; Email: rvinayakan@gmail.com

Authors

Kulangara Sandeep − *Department of Chemistry, Government Victoria College, Research Center under University of Calicut, Palakkad 678001 Kerala, India;* orcid.org/0000-0002-4275-3495

Madhavan Shanthil − *Department of Chemistry, Government Victoria College, Research Center under University of Calicut, Palakkad 678001 Kerala, India;* orcid.org/0000-0002-6478-1155

Santhakumar Dhanya − *Department of Chemistry (Research Center under MG University, Kerala), NSS Hindu College (Nationally Accredited with 'A' Grade), Changanacherry 686102 Kerala, India*

Aravind Archana − *Department of Chemistry, Saveetha School of Engineering, SIMATS, Chennai 602105 Tamil Nadu, India;* orcid.org/0000-0002-3718-0063

Muthunayagam Vibin − *Department of Biochemistry, St. Albert's College (Autonomous), Mahatma Gandhi University, Ernakulam 682018 Kerala, India*

Hareendran Divyalakshmi − *Department of Chemistry (Research Center under MG University, Kerala), NSS Hindu College (Nationally Accredited with 'A' Grade), Changanacherry 686102 Kerala, India*

Complete contact information is available at: https://pubs.acs.org/10.1021/acsomega.3c07518

Notes

The authors declare no competing financial interest.

ACKNOWLEDGMENTS

V.R., K.S., and M.S. sincerely acknowledge the mentorship, guidance, and limitless support from Professor (Dr.) K. George Thomas, School of Chemistry, Indian Institute of Science Education and Research (IISER), Thiruvananthapuram, India, for the completion of this work. The authors thank Dr. T. R. Santhosh Kumar, Scientist, Rajiv Gandhi Centre for Biotechnology (RGCB), Thiruvananthapuram 695 014, Kerala,

India, for blood serum analysis. The authors thank Robert Philip, senior technical officer, NIIST-CSIR for helping with HRTEM studies.

DEDICATION

†Dedicated to Late Professor M. V. George.

REFERENCES

(1) Marchetti, P.; Decaudin, D.; Macho, A.; Zamzami, N.; Hirsch, T.; Susin, S. A.; Kroemer, G. Redox regulation of apoptosis: Impact of thiol oxidation status on mitochondrial function. *Eur. J. Immunol.* **1997**, *27*, 289−296.
(2) Yang, J.; Carroll, K. S.; Liebler, D. C. The expanding landscape of the thiol redox proteome. *Mol. Cell Proteomics* **2016**, *15*, 1−11.
(3) Murphy, M. P.; Bayir, H.; Belousov, V.; et al. Guidelines for measuring reactive oxygen species and oxidative damage in cells and in vivo. *Nat. Metab.* **2022**, *4*, 651−662.
(4) Paulsen, C. E.; Carroll, K. S. Cysteine-mediated redox signaling: chemistry, biology, and tools for discovery. *Chem. Rev.* **2013**, *113*, 4633−4679.
(5) Seshadri, S.; Beisar, A.; Selhub, J.; Jacques, P. F.; Rosenberg, V.; D'Agostino, R. B.; Wilson, P. W. F.; Wolf, P. A. Plasma homocysteine as a risk factor for dementia and Alzheimer's disease. *N. Engl. J. Med.* **2002**, *346*, 476−483, DOI: 10.1056/nejmoa011613.
(6) Hasan, T.; Arora, R.; Bansal, A. K.; Bhattacharya, R.; Sharma, G. H.; Singh, L. R. Disturbed homocysteine metabolism is associated with cancer. *Exp. Mol. Med.* **2019**, *51*, 1−13.
(7) Balendiran, G. K.; Dabur, R.; Fraser, D. The role of glutathione in cancer. *Cell Biochem. Funct.* **2004**, *22*, 343−352.
(8) Meister, A. Selective modification of glutathione metabolism. *Science* **1983**, *220* (4596), 472−477.
(9) White, P. C.; Lawrence, N. S.; Davis, J.; Compton, R. G. Electrochemical determination of thiols: A Perspective. *Electroanalysis* **2002**, *14*, 89−98.
(10) Mostafa, I. M.; Liu, H.; Hanif, S.; Rehan, M.; Gilani, H. S.; Guan, Y.; Xu, G. Synthesis of a novel electrochemical probe for the sensitive and selective detection of biothiols and its clinical applications. *Anal. Chem.* **2022**, *94* (18), 6853−6859.
(11) Li, Z.; Liu, M.; Chen, C.; Pan, Y.; Cui, X.; Sun, J.; Zhao, F.; Cao, Y. Simultaneous determination of serum homocysteine, cysteine, and methionine in patients with schizophrenia by liquid chromatography−tandem mass spectrometry. *Biomed. Chromatogr.* **2022**, *36* (6), No. e5366.
(12) Zhang, W.; Li, P.; Geng, Q.; Duan, Y.; Guo, M.; Cao, Y. Simultaneous determination of glutathione, cysteine, homocysteine, and cysteinylglycine in biological fluids by ion-pairing high-performance liquid chromatography coupled with precolumn derivatization. *J. Agric. Food Chem.* **2014**, *62* (25), 5845−5852.
(13) Kubalczyk, P.; Bald, E.; Furmaniaka, P.; Głowacki, R. Simultaneous determination of total homocysteine and cysteine in human plasma by capillary zone electrophoresis with pH-mediated sample stacking. *Anal. Methods* **2014**, *6*, 4138−4143.
(14) Sasaki, Y.; Lyu, X.; Kubota, R.; Takizawa, S.; Minami, T. Easy-to-prepare mini-chemosensor array for simultaneous detection of cysteine and glutathione derivatives. *ACS Appl. Bio Mater.* **2021**, *4* (3), 2113−2119.
(15) Niu, L.-Y.; Chen, Y.-Z.; Zheng, H.-R.; Wu, L.-Z.; Tung, C.-H.; Yang, Q.-Z. Design strategies of fluorescent probes for selective detection among biothiols. *Chem. Soc. Rev.* **2015**, *44*, 6143−6160.
(16) Zhang, F.; Chen, F.; Shen, R.; Chen, Y.; Zhao, Z.; Zhang, B.; Fang, J. Naphthalimide fluorescent skeleton for facile and accurate quantification of glutathione. *Anal. Chem.* **2023**, *95* (9), 4301−4309.
(17) Kaushik, R.; Nehra, N.; Novakova, V.; Zimcik, P. Near-infrared probes for biothiols (Cysteine, Homocysteine, and Glutathione): A comprehensive review. *ACS Omega* **2023**, *8*, 98−126.
(18) Guo, J.; Kuai, Z.; Zhang, Z.; Yang, Q.; Shan, Y.; Li, Y. S. Y. A simple colorimetric and fluorescent probe with high selectivity towards cysteine over homocysteine and glutathione. *RSC Adv.* **2017**, *7*, 18867−18873.
(19) Tian, M.; Yang, M.; Liu, Y.; Jiang, F.-L. Rapid and reversible reaction-based ratiometric fluorescent probe for imaging of different glutathione levels in living cells. *ACS Appl. Bio Mater.* **2019**, *2* (10), 4503−4514.
(20) Bej, S.; Hazra, A.; Das, R.; Saha, S. K.; Corbella, M.; Banerjee, P. Exploratory studies of a multidimensionally talented simple Mn^{II}-based porous network: selective "turn-on" recognition@cysteine over homocysteine with an indication of cystinuria and renal dysfunction. *New J. Chem.* **2020**, *44*, 14712−14722.
(21) Zhang, Y.; Wang, D.; Meng, Y.; Lu, W.; Shuang, S.; Dong, C. Biodegradable fluorescent SiO_2@MnO_2-Based sequence strategy for glutathione sensing in a biological system and synergistic theragnostics to cancer cells. *ACS Sustainable Chem. Eng.* **2021**, *9* (7), 2770−2783.
(22) Bej, S.; Das, R.; Kundu, D.; Pal, T. K.; Banerjee, P. A de novo strategy for the development of a Zn^{II}−organic framework based luminescent "switch-on" assay for size-exclusive sensitization of the oxidised form of glutathione (GSSG) over the reduced form (GSH): insights into the sensing mechanism through DFT. *CrystEngComm* **2023**, *25*, 1626−1636.
(23) Li, H.; Wen, Y.; Zhu, X.; Wang, J.; Zhang, L.; Sun, B. Novel heterostructure of a MXene@NiFe-LDH nanohybrid with superior peroxidase-like activity for sensitive colorimetric detection of glutathione. *ACS Sustainable Chem. Eng.* **2020**, *8* (1), 520−526.
(24) Das, R.; Bej, S.; Ghosh, D.; Murmu, N. C.; Hirani, H.; Banerjee, P. Stimuli-responsive discriminative detection of Cu^{2+} and Hg^{2+} with concurrent sensing of S^{2-} from aqueous medium and bio-fluids by C-N fused azophenine functionalized "smart" hydrogel assay @A potential biomarker sensor for Wilson's disease. *Sens. Actuators, B* **2021**, *341*, No. 129925.
(25) Sudeep, P. K.; Joseph, S. T. S.; Thomas, K. G. Selective detection of cysteine and glutathione using gold nanorods. *J. Am. Chem. Soc.* **2005**, *127*, 6516−6517.
(26) Haun, J. B.; Yoon, T.-J.; Lee, H.; Weissleder, R. Magnetic nanoparticle biosensors. *WIREs Nanomed. Nanobiotechnol.* **2010**, *2*, 291−304.
(27) Baù, L.; Tecilla, P.; Mancin, F. Nanoscale Sensing with fluorescent nanoparticles. *Nanoscale* **2011**, *3*, 121−133.
(28) Feng, Y.; Song, H.; Deng, D.; Lv, Y. Engineering ratiometric persistent luminous sensor arrays for biothiols identification. *Anal. Chem.* **2020**, *92* (9), 6645−6653.
(29) Hashmi, S.; Singh, M.; Weerathunge, P.; Mayes, E. L. H.; Mariathomas, P. D.; Prasad, S. S.; Ramanathan, R.; Bansal, V. Cobalt sulfide nanosheets as peroxidase mimics for colorimetric detection of l-cysteine. *ACS Appl. Nano Mater.* **2021**, *4* (12), 13352−13362.
(30) Bu, Y.; Zhu, G.; Li, S.; Qi, R.; Bhave, G.; Zhang, D.; Han, R.; Sun, D.; Liu, X.; Hu, Z.; Liu, X. Silver nanoparticle embedded porous silicon disks enabled SERS signal amplification for selective glutathione detection. *ACS Appl. Nano Mater.* **2018**, *1* (1), 410−417.
(31) Sanskriti, I.; Upadhyay, K. K. Facile designing of a colorimetric plasmonic gold nanosensor for selective detection of cysteine over other biothiols. *ChemistrySelect* **2017**, *2* (34), 11200−11205.
(32) Chi, H.; Cui, X.; Lu, Y.; Yu, M.; Fei, Q.; Feng, G.; Shan, H.; Huan, Y. Colorimetric determination of cysteine based on Au@Pt nanoparticles as oxidase mimetics with enhanced selectivity. *Microchim. Acta* **2022**, *189*, No. 13, DOI: 10.1007/s00604-021-05091-7.
(33) Li, S.; Zhang, Q.; Lu, Y.; Zhang, D.; Liu, J.; Zhu, L.; Li, C.; Hu, L.; Li, J.; Liu, Q. Gold nanoparticles on graphene oxide substrate as sensitive nanoprobes for rapid L-cysteine detection through smartphone-based multimode analysis. *ChemistrySelect* **2018**, *3* (35), 10002−10009.
(34) Medintz, I. L.; Uyeda, H. T.; Goldman, E. R.; Mattoussi, H. Quantum dot bioconjugates for imaging, labelling and sensing. *Nat. Mater.* **2005**, *4*, 435−446.
(35) Wu, P.; Yan, X.-P. Doped quantum dots for chemo/biosensing and bioimaging. *Chem. Soc. Rev.* **2013**, *42*, 5489−5521.

https://doi.org/10.1021/acsomega.3c07518
ACS Omega 2024, 9, 6588−6594

(36) Ji, C.; Zhou, Y.; Leblanc, R. M.; Peng, Z. Recent developments of carbon dots in biosensing: A review. *ACS Sens.* **2020**, *5* (9), 2724−2741.
(37) Shellaiah, M.; Sun, K. W. Review on carbon dot-based fluorescent detection of biothiols. *Biosensors* **2023**, *13*, No. 335.
(38) Kamaci, U. D.; Kamaci, M. Selective and sensitive ZnO quantum dots based fluorescent biosensor for detection of cysteine. *J. Fluoresc.* **2021**, *31*, 401−414, DOI: 10.1007/s10895-020-02671-3.
(39) Pramanik, S.; Roy, S.; Bhandari, S. Luminescence enhancement based sensing of L-cysteine by doped quantum dots. *Chem. - Asian J.* **2020**, *15* (13), 1948−1952.
(40) Sandeep, K.; Reshmi, C. P. Modulating the Emission of $CsPbBr_3$ perovskite nanocrystals via thermally varying magnetic field of $La_{0.67}Sr_{0.33}Mn_{0.9}(Ni/Co)_{0.1}O_3$. *AIP Adv.* **2020**, *10*, No. 035302.
(41) Zhang, Y.; Li, Y.; Yan, X.-P. Photoactivated CdTe/CdSe quantum dots as a near infrared fluorescent probe for detecting biothiols in biological fluids. *Anal. Chem.* **2009**, *81* (12), 5001−5007.
(42) Sandeep, K. Revealing the role of aggregation and surface chemistry in the bi-phasic anion exchange reactions of caesium lead halide perovskites. *ChemistrySelect* **2020**, *5*, 4034−4039.
(43) Freeman, R.; Finder, T.; Bahshi, L.; Gill, R.; Willner, I. Functionalized CdSe/ZnS QDs for the detection of nitroaromatic or RDX explosives. *Adv. Mater.* **2012**, *24*, 6416−6421.
(44) Mu, Q.; Li, Y.; Ma, Y.; Zhong, X. Visual detection of biological thiols based on lightening quantum dot−TiO_2 composites. *Analyst* **2014**, *139*, 996−999.
(45) Chang, D.; Zhao, Z.; Li, W.; Shi, H.; Yang, Y.; Shi, L.; Shuang, S. Hg^{2+}-Mediated ratiometric fluorescent carbon dots for imaging glutathione in living cells and zebrafish. *ACS Sustainable Chem. Eng.* **2022**, *10* (30), 10068−10076.
(46) Das, R.; Pal, R.; Bej, S.; Mondal, M.; Kundu, K.; Banerjee, P. Recent progress in 0D optical nanoprobes for applications in the sensing of (bio)analytes with the prospect of global health monitoring and detailed mechanistic insights. *Mater. Adv.* **2022**, *3*, 4421−4459.
(47) Li, M.; Chen, T.; Gooding, J. J.; Liu, J. Review of carbon and graphene quantum dots for sensing. *ACS Sens.* **2019**, *4* (7), 1732−1748.
(48) Liu, W.; Chen, J.; Xu, Z. Fluorescent probes for biothiols based on metal complex. *Coord. Chem. Rev.* **2021**, *429*, No. 213638.
(49) Dhenadhayalan, N.; Lin, T.-W.; Lee, H.-L.; Lin, K.-C. Multisensing capability of $MoSe_2$ quantum dots by tuning surface functional groups. *ACS Appl. Nano Mater.* **2018**, *1* (7), 3453−3463.
(50) Kumar, A. S. K.; Tseng, W.-B.; Wu, M.-J.; Huang, Y.-Y.; Tseng, W.-L. L-cystine-linked BODIPY-adsorbed monolayer MoS_2 quantum dots for ratiometric fluorescent sensing of biothiols based on the inner filter effect. *Anal. Chim. Acta* **2020**, *1113*, 43−51.
(51) Sławski, J.; Białek, R.; Burdziński, G.; Gibasiewicz, K.; Worch, R.; Grzyb, J. Competition between photoinduced electron transfer and resonance energy transfer in an example of substituted cytochrome c−quantum dot systems. *J. Phys. Chem. B* **2021**, *125* (13), 3307−3320.
(52) Zhu, H.; Yang, Y.; Wu, K.; Lian, T. Charge transfer dynamics from photoexcited semiconductor quantum dots. *Annu. Rev. Phys. Chem.* **2016**, *67*, 259−281.
(53) Tan, J.; Peng, B.; Tang, L.; Zeng, G.; Lu, Y.; Wang, J.; Ouyang, X.; Zhu, X.; Chen, Y.; Feng, H. CuS QDs/Co_3O_4 polyhedra-driven multiple signal amplifications activated h-BN photoeletrochemical biosensing platform. *Anal. Chem.* **2020**, *92* (19), 13073−13083.
(54) Li, Z.; Lu, J.; Wei, W.; Tao, M.; Wang, Z.; Dai, Z. Recent advances in electron manipulation of nanomaterials for photo-electrochemical biosensors. *Chem. Commun.* **2022**, *58*, 12418−12430.
(55) Harvie, A. J.; Smith, C. T.; Ahumada-Lazo, R.; Jeuken, L. J. C.; Califano, M.; Bon, R. S.; Hardman, S. J. O.; Binks, D. J.; Critchley, K. Ultrafast trap state-mediated electron transfer for quantum dot redox sensing. *J. Phys. Chem. C* **2018**, *122* (18), 10173−10180.
(56) Xue, S.; Jiang, X.-F.; Zhang, G.; Wang, H.; Li, Z.; Hu, X.; Chen, M.; Wang, T.; Luo, A.; Ho, H.-P.; He, S.; Xing, X. Surface plasmon-enhanced optical formaldehyde sensor based on CdSe@ZnS quantum dots. *ACS Sens.* **2020**, *5* (4), 1002−1009.
(57) Linkov, P. A.; Vokhmintcev, K. V.; Samokhvalov, P. S.; et al. Effect of the semiconductor quantum dot shell structure on fluorescence quenching by acridine ligand. *JETP Lett.* **2018**, *107*, 233−237.
(58) Serrano, I. C.; Vazquez-Vazquez, C.; Adams, A. M.; Stoica, G.; Correa-Duarte, M. A.; Palomares, E.; Alvarez-Puebla, R. A. The effect of the silica thickness on the enhanced emission in single particle quantum dots coated with gold nanoparticles. *RSC Adv.* **2013**, *3*, 10691−10695.
(59) Ji, B.; Giovanelli, E.; Habert, B.; et al. Non-blinking quantum dot with a plasmonic nanoshell resonator, non-blinking quantum dot with a plasmonic nanoshell resonator. *Nat. Nanotechnol.* **2015**, *10*, 170−175.
(60) Bagheri, E.; Ansari, L.; Abnous, K.; Taghdisi, S. M.; Ramezani, P.; Ramezani, M.; Alibolandi, M. Silica-quantum dot nanomaterials as a versatile sensing platform. *Crit. Rev. Anal. Chem.* **2020**, 687−708.
(61) Algar, W. R.; Massey, M.; Rees, K.; et al. Photoluminescent nanoparticles for chemical and biological analysis and imaging. *Chem. Rev.* **2021**, *121* (15), 9243−9358.
(62) Vinayakan, R.; Shanmugapriya, T.; Nair, P. V.; Ramamurthy, P.; Thomas, K. G. An approach for optimizing the shell thickness of core−shell quantum dots using photoinduced charge transfer. *J. Phys. Chem. C* **2007**, *111* (28), 10146−10149.
(63) Vibin, M.; Vinayakan, R.; John, A.; Raji, V.; Rejiya, C. S.; Vinesh, N. S.; Abraham, A. Cytotoxicity and fluorescence studies of silica-coated CdSe quantum dots for bioimaging applications. *J. Nanopart. Res.* **2011**, *13*, 2587−2596.
(64) Lakowicz, J. R. *Principles of Fluorescence Spectroscopy*, 3rd ed.; Springer: Singapore, 2010.
(65) Billone, P. S.; Maretti, L.; Maurel, V.; Scaiano, J. C. Dynamics of the dissociation of a disulfide biradical on a CdSe nanoparticle surface. *J. Am. Chem. Soc.* **2007**, *129*, 14150−14151.
(66) Wuister, S. F.; Donegá, C. M.; Meijerink, A. Influence of thiol capping on the exciton luminescence and decay kinetics of CdTe and CdSe quantum dots. *J. Phys. Chem. B* **2004**, *108*, 17393−17397.
(67) Jeong, S.; Achermann, M.; Nanda, J.; Ivanov, S.; Klimov, V. I.; Hollingsworth, J. A. Effect of the thiol−thiolate equilibrium on the photophysical properties of aqueous CdSe/ZnS nanocrystal quantum dots. *J. Am. Chem. Soc.* **2005**, *127*, 10126−10127.
(68) Sengupta, S.; Wehbe, C.; Majors, A. K.; Ketterer, M. E.; DiBello, P. M.; Jacobsen, D. W. Relative roles of albumin and ceruloplasmin in the formation of homocysteine, homocysteine-cysteine-mixed disulfide, and cystine in circulation. *J. Biol. Chem.* **2001**, *276*, 46896−46904.
(69) Benesch, R. E.; Benesch, R. The acid strength of the -SH group in cysteine and related compounds. *J. Am. Chem. Soc.* **1955**, *77*, 5877−5881.
(70) Niu, H.; Liu, J.; O'Connor, H. M.; Gunnlaugsson, T.; James, T. D.; Zhang, H. Photoinduced electron transfer (PeT) based fluorescent probes for cellular imaging and disease therapy. *Chem. Soc. Rev.* **2023**, *52*, 2322−2357.
(71) Kundu, B.; Chakrabarti, S.; Pal, A. Redox levels of dithiols in II−VI quantum dots vis-à -vis photoluminescence quenching: Insight from scanning tunneling spectroscopy. *Chem. Mater.* **2014**, *26*, 5506−5513.
(72) Olshansky, J. H.; Ding, X. T.; Lee, Y. V.; Leone, S. R.; Alivisatos, A. P. Hole transfer from photoexcited quantum dots: the relationship between driving force and rate. *J. Am. Chem. Soc.* **2015**, *137* (49), 15567−15575.
(73) Mirzahosseini, A.; Noszál, B. Species-specific standard redox potential of thiol-disulfide systems: a key parameter to develop agents against oxidative stress. *Sci. Rep.* **2016**, *6*, No. 37596.

https://doi.org/10.1021/acsomega.3c07518
ACS Omega 2024, 9, 6588−6594